Preparation of FeCoNiWMoCr High-Entropy Alloy Coatings Via Double Glow Plasma Surface Alloying Technology

Chong Liu, Chenglei Wang,, Chaojie Liang, Xin Li, Hu Chen, Zhujiang Tan,Jingya Zhang, Mei Huang & Yatao Zhu*

ABSTRACT

In this work, the FeCoNiWMoCr high-entropy alloy (HEA) gradient coatings metallurgically bonded to the substrate was successfully prepared using double glow plasma surface alloying technology (DGPSAT) under vacuum conditions. The HEA coating was then aged at 900 ℃ for 2 h. The microstructure, elemental distribution, mechanical properties, and tribology properties of the HEA coatings was systematically studied. The results showed that the coatings consists of the σ phase, hexagonal closed-packed phase, and face-centered cubic phase, with gradient distribution and uniform elemental composition. The properties of the HEA coating after aging treatment are greatly improved compared with those before aging treatment. The HEA coating after aging treatment exhibits good bonding strength with the substrate with a bonding force of 51.4 N. The microhardness is 802 HV, which is nearly 7.5 times higher than that of the substrate. The wear amount is 2×10^{-3} mm^3, almost 6.5 times higher than that of the substrate. The wear mechanism of the HEA coatings is abrasive wear with oxidation wear and adhesive wear. DGPSAT is a practical and useful method for preparing HEA coatings with high hardness and good wear resistance.

Keywords: HEA coating; DGPSAT; aging treatment; hardness; tribology properties.

Classification: FoR Code: 0913

Language: English

Great Britain Journals Press

LJP Copyright ID: 925621
Print ISSN: 2631-8490
Online ISSN: 2631-8504

London Journal of Research in Science: Natural and Formal

Volume 24 | Issue 4 | Compilation 1.0

Preparation of FeCoNiWMoCr High-Entropy Alloy Coatings Via Double Glow Plasma Surface Alloying Technology

Chong Liu[α], Chenglei Wang[σ, *], Chaojie Liang[ρ], Xin Li[ↀ], Hu Chen[¥], Zhujiang Tan [§], Jingya Zhang [χ], Mei Huang [ν] & Yatao Zhu[Θ]

ABSTRACT

In this work, the FeCoNiWMoCr high-entropy alloy (HEA) gradient coatings metallurgically bonded to the substrate was successfully prepared using double glow plasma surface alloying technology (DGPSAT) under vacuum conditions. The HEA coating was then aged at 900 ℃ for 2 h. The microstructure, elemental distribution, mechanical properties, and tribology properties of the HEA coatings was systematically studied. The results showed that the coatings consists of the σ phase, hexagonal closed-packed phase, and face-centered cubic phase, with gradient distribution and uniform elemental composition. The properties of the HEA coating after aging treatment are greatly improved compared with those before aging treatment. The HEA coating after aging treatment exhibits good bonding strength with the substrate with a bonding force of 51.4 N. The microhardness is 802 HV, which is nearly 7.5 times higher than that of the substrate. The wear amount is 2×10^{-3} mm^3, almost 6.5 times higher than that of the substrate. The wear mechanism of the HEA coatings is abrasive wear with oxidation wear and adhesive wear. DGPSAT is a practical and useful method for preparing HEA coatings with high hardness and good wear resistance.

Keywords: HEA coating; DGPSAT; aging treatment; hardness; tribology properties.

Author α σ ↀ ¥ § χ ν,Θ: School of Materials Science and Engineering, and Guangxi Key Laboratory of Information Materials, and Engineering Research Center of Electronic Information Materials and Devices, Ministry of Education, Guilin University of Electronic Technology, Guilin 541004, P.R. China.
ρ: School of Materials Science and Engineering, Central South University, Hunan, Changsha 410083, P.R. China.

I. INTRODUCTION

Fe and steel materials are important resources that are essential for national construction. They are characterized by high strength, good plasticity and toughness, and easy processing. However, their use has resulted in a large amount of economic losses due to the effects of fracture, corrosion, wear and deformation, and premature failure of materials. Material failure frequently starts on the surface [1-2], and modifying the surface of materials can considerably improve the performance and lifetime of materials, while simultaneously reducing the amount of alloys used and economic costs. Accordingly, material surface modification technologies are widely used at present [3-5].

Double glow plasma surface alloying technology (DGPSAT) is a surface modification technology that has been extensively used in aerospace, biomedicine, and many other fields in recent years and has attracted widespread attention [6-9]. This technology uses low- temperature plasma generated by glow or arc discharge to form alloy coatings on a material surface under vacuum conditions [10-11]. It can be used to prepare high-performance surface-modified coatings on the surface of workpieces with various

London Journal of Research in Science: Natural and Formal

complex shapes, and the coating is metallurgically bonded to the substrate, achieving controlled composition and good structural characteristics [12-13].

DGPSAT can allow the combination of Ni, W, Co, Mo, Cr, and other metal elements to infiltrate into steel materials and various metal surfaces to form alloy coatings with excellent properties. Huang et al. [14] prepared a Cr–Ni alloy coating on the surface of Q235 low-C steel via DGPSAT, and the highest protection efficiency of this alloy coating in 3.5% NaCl corrosion solution reached 99.23%, effectively improving the corrosion resistance of Q235. Qiu et al. [15] prepared a dense W–Mo layer on gear steel by using DGPSAT, and the specific wear rates of the coating were 11.2×10^{-5} $mm^3\cdot N^{-1}\cdot m^{-1}$ and 8.1×10^{-5} $mm^3\cdot N^{-1}\cdot m^{-1}$ at high temperature and room temperature, respectively, which was 19% of that of the substrate, significantly improving the wear resistance of the gear steel. Liu et al. [16] prepared a multi-alloy layer that contained Cr, Co, Mo, and Ni on the surface of pure Fe via DGPSAT and then aged this layer. The results showed that the alloy layer formed using the appropriate aging treatment exhibited better wear resistance than stainless steel. Numerous studies have shown that the metal elements Co, Ni, W, Mo, and Cr can form a good solid solution in steel materials and penetrate well into the substrate, improving the properties of the material surface. At present, however, surface-modified alloy coatings prepared via DGPSAT are mostly based on traditional alloys, and research on the preparation of new high-entropy alloy (HEA) coatings is minimal. In recent years, HEAs have become a research hotspot because of their better performance than traditional alloys. He et al. [17] prepared $(FeCoNiCr)_{94}Ti_2Al_4$ HEA with tensile strength up to 900 MPa and ductility up to 40% under aging treatment at 800 ℃. Tong et al. [18] prepared FeCoNiCrTi0.2 HEA and strengthened it with precipitation. Their results showed that the yield strength of the precipitation-strengthened HEA increased from 700 MPa to 860 MPa compared with that before strengthening. Varun et al. [19] studied the influence of different Cu contents on the magnetic properties of FeCoNiCrCu(x) HEA, and their results indicated that saturation magnetization intensity increased from 30.7 emu/g to 32.7 emu/g when Cu content was increased from 0 to 0.5. Numerous studies have demonstrated that the FeCoNiWMoCr system of HEAs has excellent mechanical properties, a wide range of applications, and good prospects for application. Compared with bulk HEA, HEA coatings have fewer organizational defects and can significantly improve the performance of the material surface, reduce the amount of alloy used, and decrease economic costs. HEA coating exhibits the same four effects of block HEA, but is better than block HEA in terms of performance [20-22].

Notably, in conventional DGPSAT, the surface alloy coatings prepared on steel materials are solid solution diffusion layers with the base element as the primary element. Simultaneously, solid solution diffusion layers cannot form HEA coatings with multiple dominant elements. Therefore, this study is designed to prepare a gradient HEA coating with a deposited layer + diffusion layer via DGPSAT.

In this study, we will break the idea of preparing traditional alloy-modified coatings on steel materials via DGPSAT and prepare a new gradient FeCoNiWMoCr HEA coating that is metallurgically bonded to the substrate via Co–Ni–W–Mo–Cr five-element co-diffusion on pure Fe surface and then perform aging treatment on it. The structure and elemental composition distribution of the HEA coating before and after aging treatment were analyzed. Bond strength, hardness, and wear resistance were systematically studied to provide a reference for the study of HEA coating preparation via DGPSAT.

II. EXPERIMENTAL METHOD

2.1 Preparation of FeCoNiWMoCr HEA coatings

In this work, the DGLT-15F multifunctional ion chemical heat treatment furnace was used to carry out Co-Ni-W-Mo-Cr five elements co-infiltration on the surface of pure iron under vacuum conditions to obtain FeCoNiWMoCr HEA coating. The base material is pure iron (purity >99.9%, size: 100 mm×15

mm×2 mm), the target material is pure Co, Ni, W, Mo, Cr bar target (purity ≥99.9%, size: ⌀4 mm×40 mm), the quantity ratio is Co: Ni: W: Mo: Cr = 35:65:11:11:65. The source level bar target is uniformly inserted into a hollow circular barrel (size: ⌀130 mm×180 mm) prepared from carbon steel, and the workpiece is suspended in the center of the circular barrel with a hook, and at the same time, the workpiece is connected to the source power supply through the hook, so as to achieve the effect of controlling the voltage of the source level and the voltage of the workpiece with a single power supply at the same time, and to form an equipotential effect between the source level and the workpiece. The process parameters of the test are as follows: pole spacing, 30mm, workpiece gas pressure 30Pa (at Ar atmosphere, purity ≥99.99%), voltage 850V, holding temperature 1300°C, holding time 2h. Holding at high temperatures, after the end of the holding time with the furnace slowly cooled down to room temperature, to obtain the HEA coatings (hereinafter referred to as C1), the use of high temperature chamber muffle furnaces SGM-M6/14 to the obtained HEA double glow plasma surface gold treatment. The SGM-M6/14 high-temperature chamber muffle furnace was used to carry out aging treatment on the obtained high-entropy alloy double-glow plasma surface treatment layer to obtain the HEA coating after aging treatment (hereinafter referred to as C2), and the aging treatment was carried out under the following process conditions: temperature of 900°C and time of 2h.

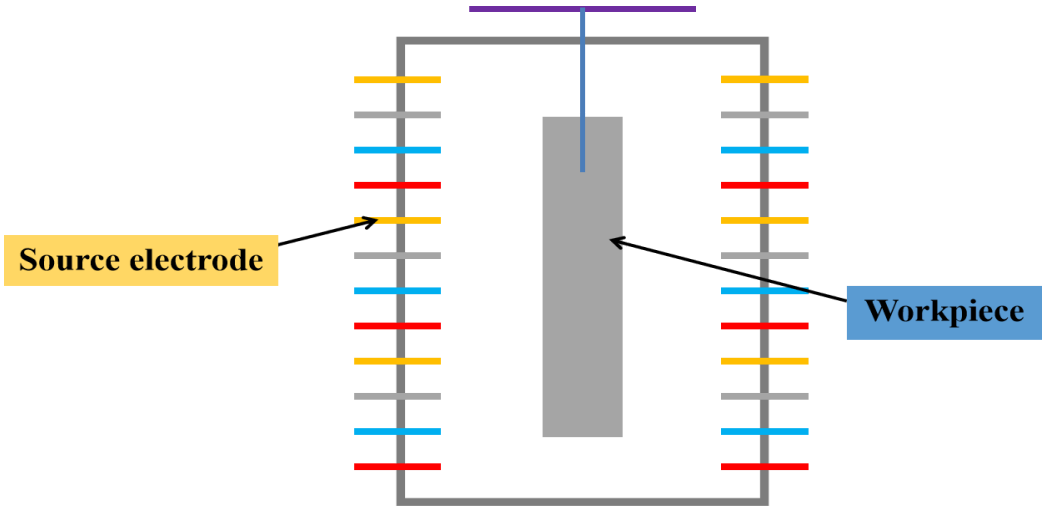

Fig.1: Schematic diagram of the spatial structure of the workpiece and source electrode.

2.2 Testing and analysis of FeCoNiWMoCr HEA coatings

The topography and composition of the surface and cross section of FeCoNiWMoCr HEA coatings were analyzed via scanning electron microscopy (SEM, JSM-IT800, JEOL Ltd.). The physical phase structure of the HEA coatings was analyzed via X-ray diffraction (XRD, Bruker D8 ADVANCE X). The hardness testing of the HEA coatings was performed using a microhardness tester (HV-1000, Shenzhen Haoxinda Instrument Co., Ltd.). The hardness values of the HEA coatings were measured at 10 locations and then averaged. A coating adhesion automatic scratch tester (WS-2005, Lanzhou Zhongke Kaihua Technology development Co., Ltd.) was utilized to test the coating bond strength of the HEA coatings by using acoustic emission signals, dynamic loading of up to 100 N, a loading rate of 100 N/min, and a scratch length of 5 mm. A 3D laser microscope (OLS4100 3D, OLYMPUS Ltd.) and a high-temperature reciprocating friction and wear tester (MGG-02, Jinan Yihua Tribology Testing Technology Co., Ltd.) were used to examine the friction and wear properties of the HEA coatings. The friction substrate was a 6 mm-diameter Si_3N_4 ball, the load was 600 g, the back-and-forth distance was 5 mm, the frequency was 300 r/min, and test time was 60 min.

III. RESULTS AND DISCUSSION

3.1 Surface appearance and element distribution of FeCoNiWMoCr HEA coatings

The surface morphology of FeCoNiWMoCr HEA coatings before and after aging treatment is shown in Fig. 2. It can be seen that surface of the HEA coatings is flat and dense, without apparent holes and cracks, and the surface denseness of C2 is better. The composition content (at.%) of the energy-dispersive X-ray spectroscopy (EDS) at the marker points of the HEA coatings and the calculated mixed entropy values are provided in Table 1. In accordance with the results, on the one hand, the composition of the HEA coatings is uniform without major differences and elemental contents are all between 5 at.% and 35 at.%. On the other hand, the molar mixed entropy of HEA with the isoatomic ratio alloy in solid-solution state is calculated as

$$\Delta S_{conf} = R \ln ln\, n \tag{1}$$

where ΔS_{conf} is the mixed entropy value ($J \cdot K^{-1} \cdot mol^{-1}$), R is the gas constant 8.314 ($J \cdot K^{-1} \cdot mol^{-1}$), and n is the component content (at.%).

The mixed entropy value calculated using Equation (1) is shown in Table 1. The mixed entropy value at each point is greater than the definition of HEA of 12.47 $J \cdot K^{-1} \cdot mol^{-1}$, and the FeCoNiWMoCr HEA coatings were successfully prepared on the surface of Fe. Interestingly, the quantity ratio of Mo and W is relatively low, but the content in the HEA coatings is relatively high. Meanwhile, the quantity ratio of Ni and Cr is relatively high, but the content in the HEA coatings is relatively low. This result is attributed to the use of the isotropic mode in this experimental procedure and the anti-sputtering influence on the substrate surface under vacuum conditions. Under the bombardment of 100 eV Ar^{+}, the sputtering parameters of the Fe, Co, Ni, W, Mo, and Cr elements [23] are provided in Table 2. The sputtering queues of the five elements are relatively low and exhibit good sputtering performance. Ni and Cr elements have higher sputtering rates. They are easily sputtered onto the substrate surface, but are also more susceptible to the back-sputtering effect and being back-sputtered out. Meanwhile, W and Mo have lower sputtering rates and are less affected by the back-sputtering effect. They are more easily deposited onto the surface of Fe. The atomic radii of the Cr and Ni do not differ considerably from the atomic radius of the substrate Fe, and thus, they are more easily diffused into the substrate. Meanwhile, the atomic radii of the Mo and W elements differ considerably from the atomic radius of the substrate Fe, and thus, they are relatively difficult to diffuse into the interior of the substrate.

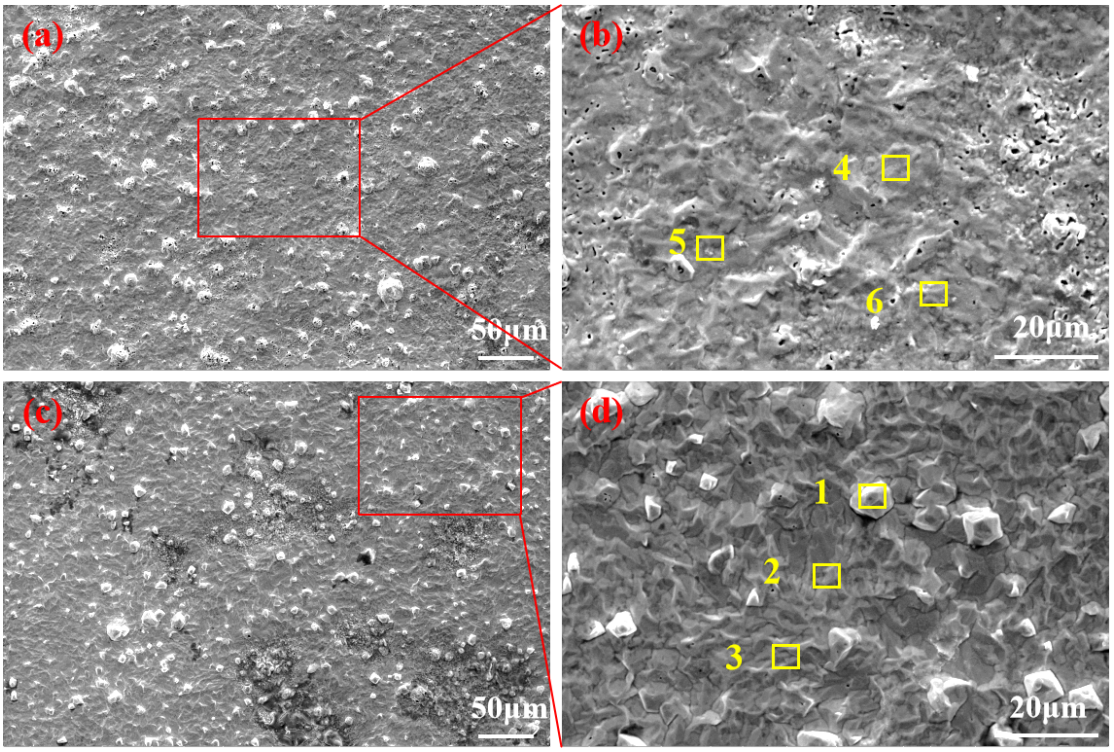

Fig.2: Surface morphology of FeCoNiWMoCr HEA coatings before and after aging treatment, (a)C1, (b)C2, (c) Partial magnification of (a), (d) Partial magnification of (b).

Table 1: EDS at the marker points of FeCoNiWMoCr HEA coatings before and after aging treatment and the calculated mixed entropy values.

Elements	Fe	Co	Ni	W	Mo	Cr	$\triangle S_{mix}$
1	20.68	9.44	6.97	33.79	20.64	8.48	13.55
2	24.64	9.35	7.34	32.19	18.2	8.29	13.71
3	22.8	8.78	7.22	32	21.19	8.05	13.64
average	22.71	9.19	7.18	32.66	20.01	8.27	13.63
4	21.72	9.26	7.05	32.56	19.60	8.35	13.56
5	23.65	8.98	7.37	32.08	20.76	8.32	13.70
6	24.39	9.15	7.19	32.38	21.03	8.15	13.71
average	23.25	9.13	7.20	32.34	20.46	8.27	13.66

Table 2: Sputtering threshold and sputtering rate of the Fe, Co, Ni, W, Mo, and Cr element under 100 eV Ar+ bombardment.

Elements	Fe	Co	Ni	W	Mo	Cr
Sputtering threshold/eV	20	25	21	33	24	22
Sputtering rate	0.2	0.15	0.28	0.068	0.13	0.3

3.2 Cross-section appearance and element distribution of FeCoNiWMoCr HEA coatings

The cross-sectional morphology of FeCoNiWMoCr HEA coatings before and after aging treatment is shown in Fig. 3(a) and Fig. 3(b). Evidently, the deposition layer of the specimens before and after the

aging treatment is continuous and uniform. The thickness is approximately the same, i.e., all the specimens are 4–6 μm. The cross section of C2 is more dense. The source structure design used in this subject fully utilizes the hollow cathode effect between the targets and the tip discharge effect of the long strip-shaped target, considerably enhancing the sputtering volume of the source target elements. Both designs ensure sufficient sputtering deposition volume for easier deposited layer formation, while the aging treatment promotes further diffusion of each element, resulting in a denser coating.

The cross-sectional EDS face scan pattern of FeCoNiWMoCr HEA coatings before and after aging treatment is shown in Fig. 3(c) and Fig. 3(d). The EDS line scanning of the cross section of FeCoNiWMoCr HEA coatings before and after aging treatment is shown in Fig. 3(e) and Fig. 3(f). The contents of Co, Ni, and Cr are relatively high in the diffusion layer and relatively low in the deposit layer. Meanwhile, the opposite is true for W and Mo. The contents of W and Mo are relatively high in the deposit layer and relatively low in the diffusion layer. The content difference of each element in the sediment layer of C1 is large, and the content difference of each element in the diffusion layer is small, and the whole is not uniform. All the elements in the deposition layer and diffusion layer of C2 reach the state of uniform distribution, with an overall gradient distribution.

The results are because, each element has a different atomic radius, and its difficulty level in entering the diffusion layer is also different. The atomic radius of Fe, Co, Ni, W, Mo, and Cr [24] are provided in Table 3. The atomic radii of Co, Ni and Cr are not very different from the atomic radius of Fe, and thus, the resistance to diffusion into the substrate of these elements is relatively small. Meanwhile, the atomic radius of W and Mo are larger, and their resistance to diffusion into the substrate is relatively large. Therefore, these elements are easier to enrich in the deposition layer. The results are consistent with the results of Table 1. The aging treatment promotes the rediffusion of each element in the HEA coating, such that each element in the diffusion layer further diffuses into the substrate, increasing element content in the substrate. Consequently, all the elements reach a state of uniform distribution and gradient distribution.

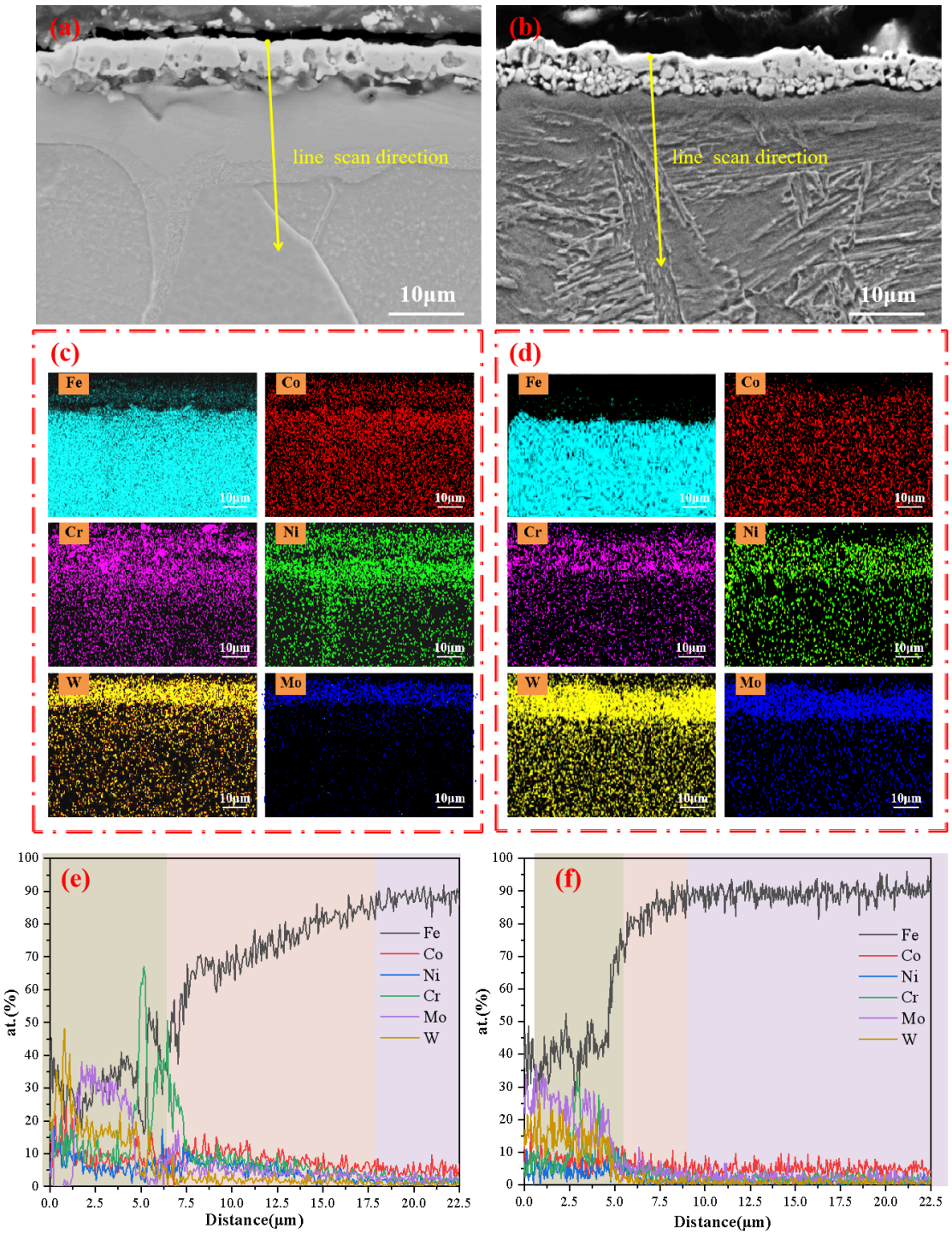

Fig.3: Cross-sectional morphology and EDS of FeCoNiWMoCr HEA coatings before and after aging treatment, (a) Cross-sectional morphology of C1, (b) Cross-sectional morphology of C2, (c) EDS face scan pattern of C1, (d) EDS face scan pattern of C2, (e) EDS Line scanning of C1, (f) EDS Line scanning of C2.

Table 3: Atomic radius of Fe, Cr, Ni, W, Mo, and Co element (Å).

Elements	Fe	Co	Ni	W	Mo	Cr
Atomic radius	1.27	1.27	1.24	1.41	1.40	1.26

3.3 Phase of FeCoNiWMoCr HEA coatings

The XRD of FeCoNiWMoCr HEA coatings before and after aging treatment is shown in Fig. 4. The coatings consist of the σ, face-centered cubic (fcc), and hexagonal closed-packed (hcp) phases. The difference between the atomic radii of Co and W in the HEA coatings is large; therefore, Mo and Co are more easily enriched, forming the Co_7W_6 phase (σ phase). The phase structure before and after aging treatment has not changed considerably.

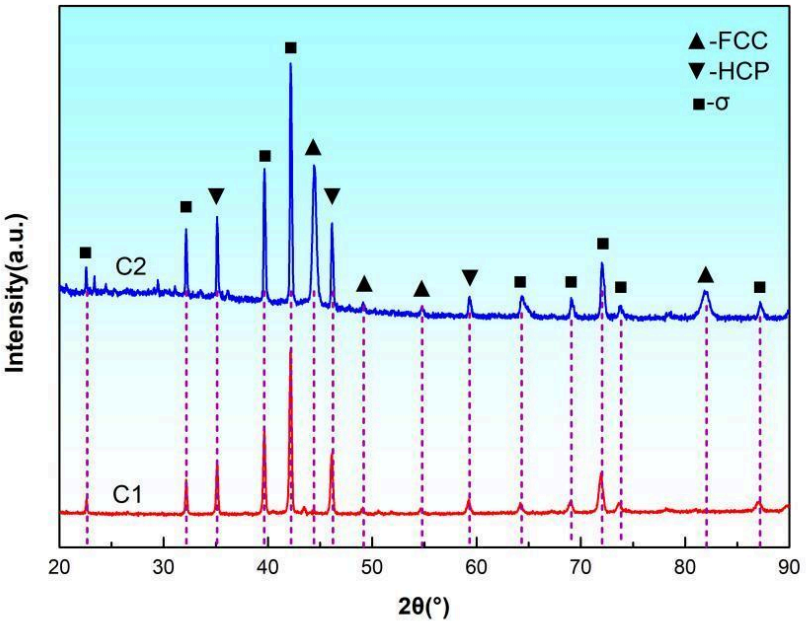

Fig.4: XRD of FeCoNiWMoCr HEA coatings before and after aging treatment.

3.4 Bonding strength of FeCoNiWMoCr HEA coatings

The acoustic emission curves and scratch morphology of FeCoNiWMoCr HEA coatings before and after aging treatment are shown in Fig. 5. It can be seen that the binding force of C1 is 42.5N and that of C2 is 51.4N. The surface morphology of the corresponding scratches shows no large area of spalling near the scratches, indicating that FeCoNiWMoCr HEA coatings achieve good toughness and its bonding with the substrate is good.

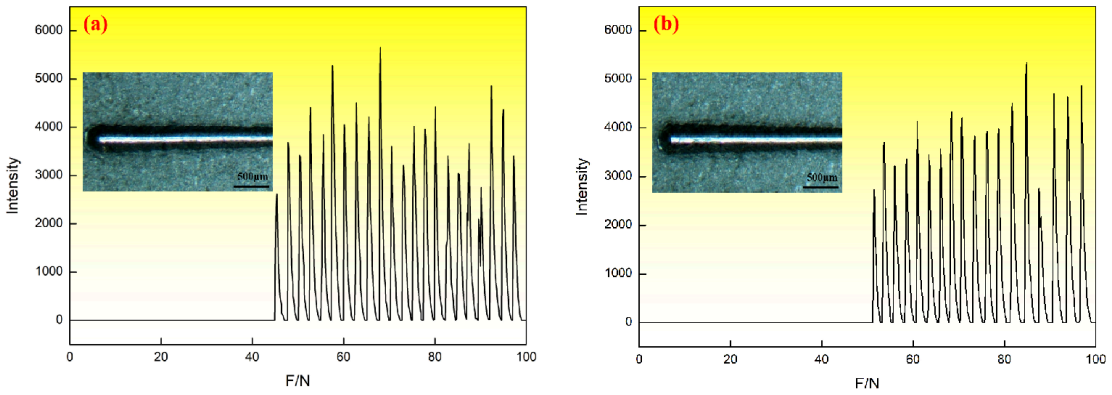

Fig.5: Acoustic emission curves and scratch morphology of FeCoNiWMoCr HEA coatings, (a) C1, (b) C2.

3.5 Microhardness and friction wear properties of FeCoNiWMoCr HEA coatings

The microhardness and wear properties of substrate Fe and FeCoNiWMoCr HEA coatings before and after aging treatment are shown in Fig. 6. From Fig. 6(b), the microhardness of FeCoNiWMoCr HEA coatings is significantly increased compared with that of substrate Fe. The microhardness of C2 is even higher, increasing from 108 HV of the substrate Fe to 802 HV, i.e., an increase of nearly 7.5 times. Surprisely, the wear of FeCoNiWMoCr HEA coatings is significantly lower compared with that of the substrate Fe, where the wear of C2 is even smaller, i.e., 2×10^{-3} mm^3, which is nearly 6.5 times higher than the 12.93×10^{-3} mm^3 of the substrate. The microhardness of FeCoNiWMoCr HEA coatings is positively correlated with friction wear performance. That is, the higher the microhardness, the better the wear resistance, the higher the microhardness of C2, the better its wear resistance.

From Fig. 6(a), it is clearly shows that the friction coefficients of substrate Fe and FeCoNiWMoCr HEA coatings enter a stable phase after a short break-in phase under friction conditions at room temperature. In the beginning of the friction sub-contact with the surface of the HEA coatings, the friction curve fluctuates more and the friction coefficient becomes unstable. As the friction continues, the friction coefficient gradually stabilizes. In the stabilization phase, the friction curve of C2 fluctuates with the gentlest amplitude. From Fig. 6(c), the wear scar surface of FeCoNiWMoCr HEA coatings is relatively flat, without large grooves, and the protrusion of the edge of the wear scar is not serious. The width and depth of the wear scar of FeCoNiWMoCr HEA coatings before and after aging treatment are clearly smaller than those of the substrate Fe, and the HEA coatings exhibit good abrasion resistance. The wear scar depth of C2 is the shallowest and demonstrates the best wear resistance.

Aging treatment improves the wear resistance of the HEA coating, because many hard and large particles are present on the surface of C1 (as shown in Fig. 1). The phenomenon of local stress concentration is more likely to occur during its friction process, such that the hard and large particles on the surface are destroyed to form hard abrasive chips that will cut the HEA coating. After aging treatment, relatively few large hard particles are present on the surface of the HEA coating. The surface is flatter, roughness is lower, and the cutting effect on the HEA coating is reduced after the formation of abrasive chips. Consequently, wear resistance is better.

The surface wear morphology of substrate Fe and FeCoNiWMoCr HEA coatings before and after aging treatment are shown in Fig. 7. The wear surface of the substrate Fe is distributed with a large amount of parallel furrows and abrasive chips, accompanied by adhesion flaking and delamination. In addition, large number of furrows and flaking pits are formed. The wear surface of FeCoNiWMoCr HEA coatings has a small amount of plow grooves and small particles of abrasive chips accompanied by shallow spalling. Its wear surface does not form evident deep grooves and spalling pits with good wear resistance. After aging treatment, the FeCoNiWMoCr HEA coating has less wear surface furrowing and more adhesive spalling.

The EDS face scans of the surface wear morphology of substrate Fe and FeCoNiWMoCr HEA coatings before and after aging treatment are shown in Fig. 8. The substrate and the HEA coatings in the friction and wear process with the friction sub exhibit different degrees of oxidation due to the heat generated during friction. Consequently, the surface is oxidized, generating a dense oxide film, which acts as a lubricant and protects the surface of the substrate and the HEA coatings, slowing down the wear on the grinding ball and improving wear resistance. The O element is the most enriched in the surface wear morphology of C2, and the formed oxide film is the thickest and exhibits the best wear resistance. In addition, the cooling method of C1 involves cooling down to room temperature with a furnace. By contrast, the cooling method of C2 is water cooling, which is equivalent to quenching treatment, improving its hardness and wear resistance. The friction sub uses Si_3N_4, and thus, the enrichment of Si elements indicates the presence of adhesive wear. The wear and tear mechanisms of substrate Fe and FeCoNiWMoCr HEA coatings is abrasive wear with oxidation wear and adhesive wear.

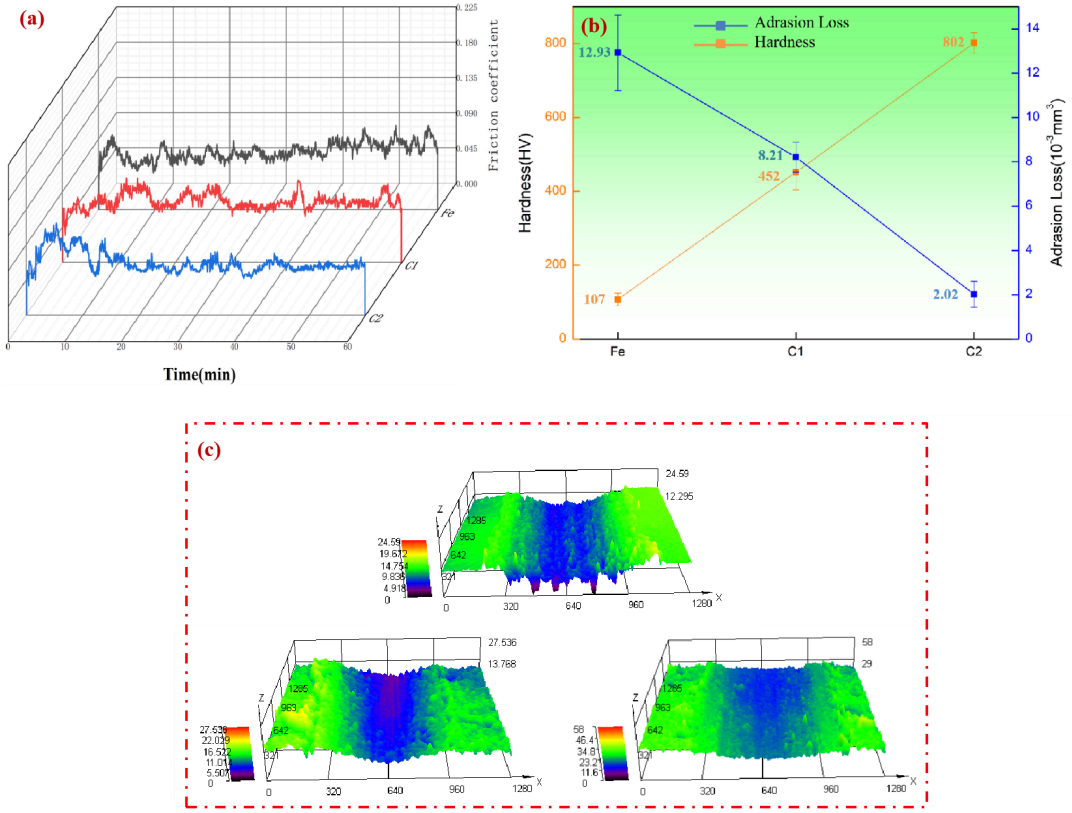

Fig.6: Microhardness and wear properties of substrate Fe and FeCoNiWMoCr HEA coatings before and after aging treatment, (a) Friction coefficient, (b) Microhardness and amount of wear, (c) Measurement of three-dimensional contour.

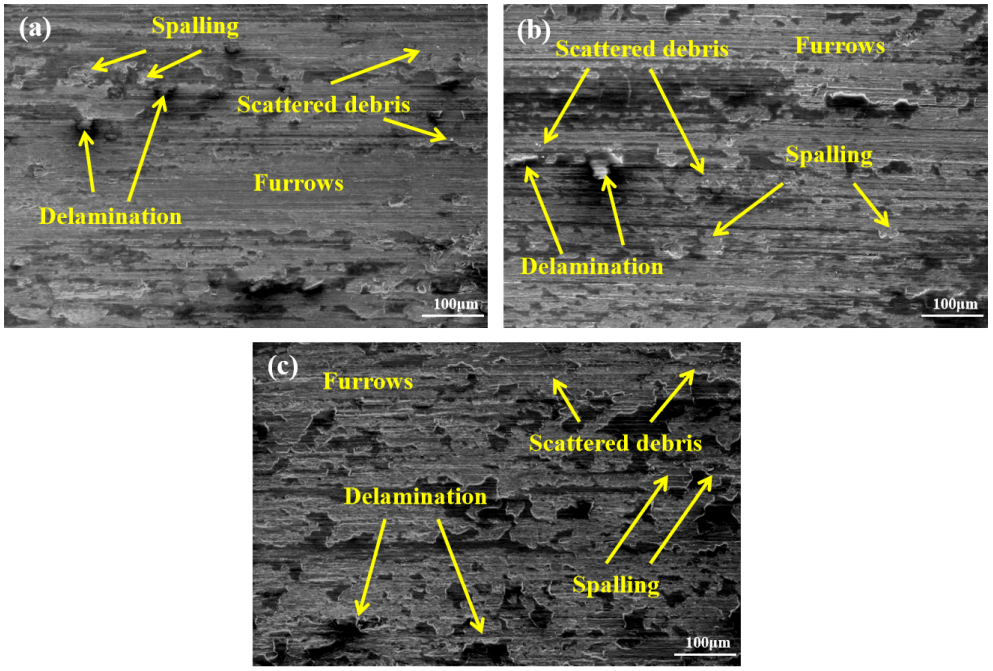

Fig.7: Surface wear morphology of substrate Fe and FeCoNiWMoCr HEA coatings before and after aging treatment, (a) C1, (b) C2, (c) Fe.

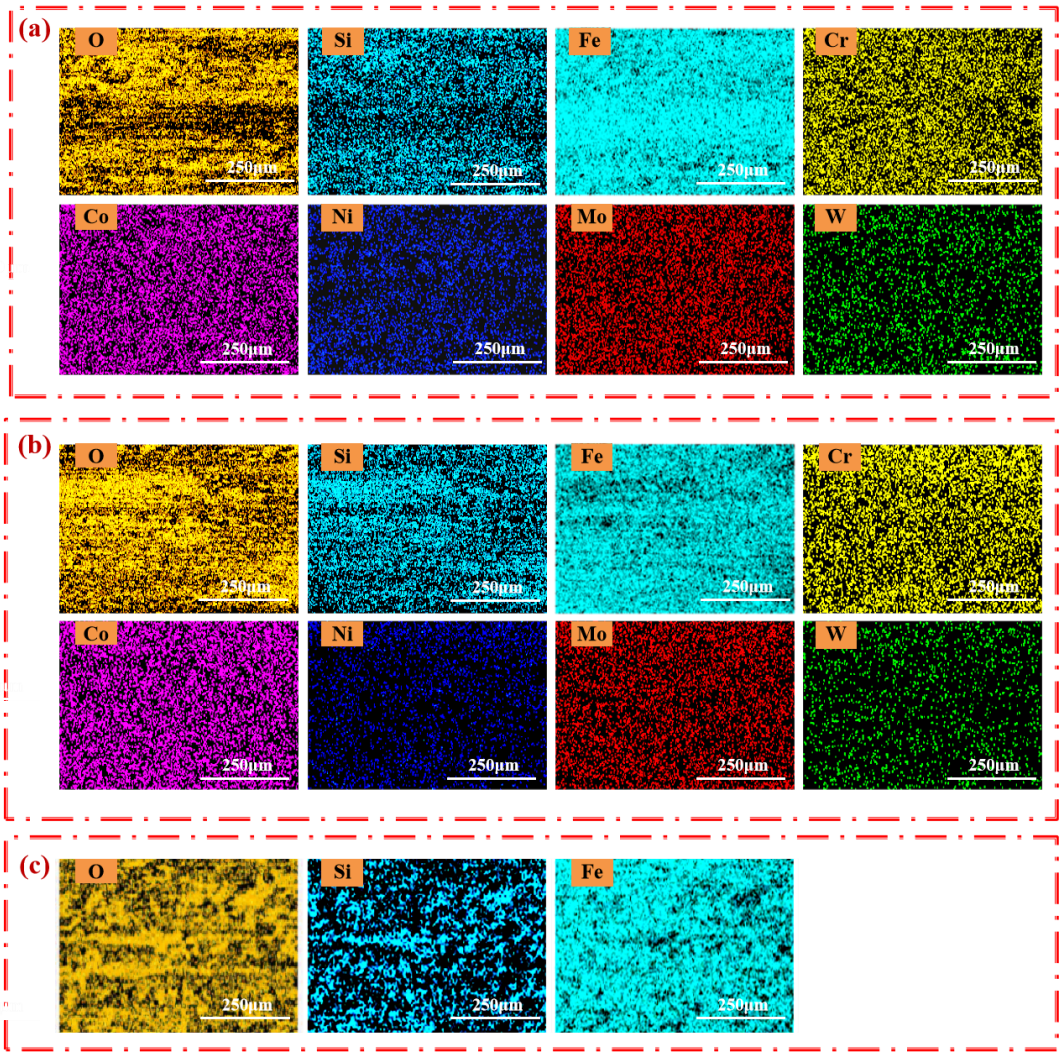

Fig.8: EDS face scans of the surface wear morphology of substrate Fe and FeCoNiWMoCr HEA coatings before and after aging treatment, (a) C1, (b) C2, (c) Fe.

IV. CONCLUSIONS

In this study, a gradient FeCoNiWMoCr HEA coating was successfully prepared on pure Fe substrate via DGPSAT, and then the coating were subjected to aging treatment. The organization, elemental composition, bond strength, microhardness, and wear properties of FeCoNiWMoCr HEA coatings before and after aging treatment were determined. The major findings are as follows.

1. The surface of FeCoNiWMoCr HEA coatings is flat and dense, and the cross section is continuous and uniform. The best quality of the HEA coatings is observed after aging treatment, forming a composite reinforced layer of deposited layer + diffusion layer. FeCoNiWMoCr HEA coatings consist of the σ, fcc, and hcp phases.
2. The bonding strength of FeCoNiWMoCr HEA coatings and the substrate is good, reaching 51.4 N after aging treatment. FeCoNiWMoCr HEA coatings effectively improve hardness, with the microhardness of the HEA coating after aging treatment reaching up to 802 HV, which is nearly 7.5 times higher than the 108 HV of the substrate.
3. FeCoNiWMoCr HEA coatings effectively improve wear resistance. The abrasion resistance of the HEA coating after aging treatment is the best, and its wear amount can be as low as 2×10^{-3} mm^3, which is nearly 6.5 times higher than the $12.93\times10^{-3}mm^3$ of the substrate. The wear and tear

mechanism of FeCoNiWMoCr HEA coatings is abrasive wear with oxidation wear and adhesive wear.

ACKNOWLEDGMENTS

This work was supported by the National Natural Science Foundation of China (52161011); the Natural Science Foundation of Guangxi Province (2023GXNSFDA026046); the Central Guiding Local Science and Technology Development Fund Projects (ZY23055005); the Scientific Research and Technology Development Program of Guilin (20220110-3, 2020010903); the Guangxi Key Laboratory of Information Materials (221024-Z, 221012-K); the Engineering Research Center of Electronic Information Materials and Devices, Ministry of Education (EIMD-AB202009); the Major Research Plan of the National Natural Science Foundation of China (92166112); and Innovation Project of GUET Graduate Education (2020YCXS118, and 2022YCXS200) for the financial support given to this work.

Data Availability

The processed data required to reproduce these findings cannot be shared at this time as the data also forms part of an ongoing study.

REFERENCES

1. Balraj Singh, Gurpreet Singh, Buta Singh Sidhu, In vitro investigation of Nb-Ta alloy coating deposited on CoCr alloy for biomedical implants, Surf. Coat. Technol 377 (2019) 124932.
2. Yan Xu, Yinfeng Wang, Yi Xu, Mingyou Li, Zheng Hu, Microscopic characteristics and properties of Fe-Based amorphous alloy compound reinforced WC-Co-Based coating via plasma spray welding, Processes 9 (2021) 6.
3. Ye Tian, Yifu Shen, Congyang Lu, Xiaomei Feng, Microstructures and oxidation behavior of Al-CrMnFeCoMoW composite coatings on Ti-6Al-4V alloy substrate via high-energy mechanical alloying method, J. Alloys Compd. 779 (2019) 456-465.
4. Chau Josepg, Lik Hang, Hou, Yen-Yu, Pan, Alfard I-Tsung, Yang, Chih-Chao, PARTICUL SCI TECHNOL 10 (2016) 209-213.
5. Chenglei Wang, Yuan Gao, Rong Wang, Deqiang Wei, Miao Cai, Yaokun Fu, Microstructure of laser-clad Ni60 cladding layers added with different amounts of rare-earth oxides on 6063 Al alloys, J. Alloys Compd. 740 (2018) 1099-1107.
6. Feng Ding, Pingze Zhang, Dongbo Wei, Xiaohu Chen, Shiyuan Wang, Zhangzhong Wang, Yimin Zhu, Isothermal oxidation behavior of Zr-Y coating on γ-TiAl by double glow plasma surface metal alloying Technique, Coatings 8 (2018) 361.
7. Naiming Lin, Junwen Guo, RuiQiang Huang, Jiaojuan Zou, Bin Tang, Double glow plasma surface alloying antibacterial silver coating on pure titanium, Surf. Rev. Lett 21 (2014) 1450032.
8. Naiming Lin, Luxia Zhang, Jiaojuan Zou, Qiang Liu, Shuo Yuan, Lulu Zhao, Yuan Yu, Zhiqi Liu, Qunfeng Zeng, Xiaoping Liu, Zhihua Wang, Bin Tang, Yuchen Wu, A combined surface treatment of surface texturing-double glow plasma surface titanizing on AISI 316 stainless steel to combat surface damage: Comparative appraisals of corrosion resistance and wear resistance, Appl. Surf. Sci 493 (2019) 747-765.
9. Dongbo Wei, Pingze Zhang, Zhengyun Yao, Jintang Zhou, Xiangfei Wei, Xiaohu Chen, Double glow plasma chromizing of Ti6Al4V alloys: Impact of working time, substrate–target distance, argon pressure and surface temperature of substrate, Vacuum 121 (2015) 81-87.
10. Zheng Ding, Qiang Miao, Wenping Liang, Zhengang Yang, Shiwei Zuo, Performance enhancement in borocarburized low-carbon steel by double glow plasma surface alloying, Coatings 10 (2020) 1205.

11. Shuo Yuan, Naiming Lin, Jiaojuan Zou, Zhiqi Liu, Zhenxia Wang, Linhai Tian, Lin Qin, Hongxia Zhang, Zhihua Wang, Bin Tang, Yucheng Wu, Effect of laser surface texturing (LST) on tribological behavior of double glow plasma surface zirconizing coating on Ti6Al4V alloy, Surf. Coat. Technol 368 (2019) 97-109.
12. Shuo Yuan, Naiming Lin, Qunfeng Zeng, Hongxia Zhang, Xiaoping Liu, Zhihua Wang, Yucheng Wu, Recent developments in research of double glow plasma surface alloying technology: a brief review, J MATER RES TECHNOL 9 (2020) 6859-6882.
13. Xixi Luo, Jing Cao, Guanghui Meng, Fangli Yu, Qiong Jiang, Pingze Zhang, Hu Xie, Double glow plasma surface metallurgy technology fabricated Fe-Al-Cr coatings with excellent corrosion resistance, Coatings 10 (2020) 575.
14. Jun Huang, Siyu Yang, Shiyu Cui, Jilin Xu, Jianping Zhang, Junming Luo, Influence of the electrode distance on microstructure and corrosion resistance of Ni-Cr alloyed layers deposited by double glow plasma surface metallurgy, J WUHAN UNIV TECHNOL 37 (2022) 1204-1215.
15. Zhongkai Qiu, Pingze Zhang, Dongbo Wei, Xiangfe Wei, Xiaohu Chen, A study on tribological behavior of double-glow plasma surface alloying W-Mo coating on gear steel, Surf. Coat. Technol 278 (2015) 92-98.
16. Xiaoping Liu, Yuan Gao, Zhonghou Li, Zhong Xu, Wenhuai Tian, Bin Tang, Cr–Ni–Mo–Co surface alloying layer formed by plasma surface alloying in pure iron, Appl. Surf. Sci 252 (2006) 3894-3902.
17. J. Y. He, H. Wang, Y. Wu, X. J. Liu, H. H. Mao, T. G. Nieh, Z. P. Lu, Precipitation behavior and its effects on tensile properties of FeCoNiCr high-entropy alloys, Intermetallics 79 (2016) 41-52.
18. Y. Tong, K. Jin, H. Bei, J. Y. P. Ko, D. C. Pagan, Y. Zhang, F. X. Zhang, Local lattice distortion in NiCoCr, FeCoNiCr and FeCoNiCrMn concentrated alloys investigated by synchrotron X-ray diffraction, MATER DESIGN 155 (2018) 1-7.
19. Varun Chaudhary, Visha Soni, Bharat Gwalani, R. V. Ramanujan, Rajarshi Banerjee, Influence of non-magnetic Cu on enhancing the low temperature magnetic properties and curie temperature of FeCoNiCrCu(x) high entropy alloys, SCRIPTA MATER 182 (2020) 99-103.
20. Linzhi Que, Guofu Lian, Mingpu Yao, Hua Lu, Microstructure and properties of AlCoCrFeNiTi high-entropy alloy coatings prepared by laser cladding based on the response surface methodology, Int. J. Adv. Manuf. Technol. 123 (2022) 1307-1321.
21. Y. K. Mu, Y. D. Jia, L. Xu, Y. F. Jia, X. H. Tan, J. Yi, G. Wang, P. K. Liaw, Nano oxides reinforced high-entropy alloy coatings synthesized by atmospheric plasma spraying, Mater. Res. Lett. 7 (2019) 312-319.
22. Michael C. Gao, Jien-Wei Yeh, Peter K. Liaw, Yong Zhang, High-entropy alloys: Fundamentals and applications, 2016.
23. Z. Xu. Plasma Surface Metallurgy, Science Press, 2007.
24. A. Takeuchi, A. Inoue, Classification of bulk metallic glasses by atomic size difference, heat of mixing and period of constituent elements and its application to characterization of the main alloying element, Mater Trans. 46 (2005) 2817-2829.

This page is intentionally left blank